Electronic Supplementary Information

Insights of the Efficient Hydrogen Evolution Reaction Performance in Bimetallic Au_4Cu_2 Nanoclusters

Aarti Devi[a], Harpriya Minhas[b], Lipipuspa Sahoo[a], Rashi[a], Saniya Gratious[c], Amitabha Das[b], Sukhendu Mandal[c], Biswarup Pathak[b*], Amitava Patra[a,d*]

[a]*Institute of Nano Science and Technology, Knowledge City, Sector 81, Mohali 14036, India*

[b]*Department of Chemistry, Indian Institute of Technology (IIT) Indore, Indore, Madhya Pradesh, 453552, India*

[c]*School of Chemistry, Indian Institute of Science Education and Research Thiruvananthapuram, Thiruvananthapuram, Kerala-695551, India*

[d]*School of Materials Sciences, Indian Association for the Cultivation of Science, Jadavpur, Kolkata-700032, India*

*Author to whom correspondence should be addressed; E-mail: msap@iacs.res.in, biswarup@iiti.ac.in, Phone: (91)-33-2473-4971, Fax: (91)-33-2473

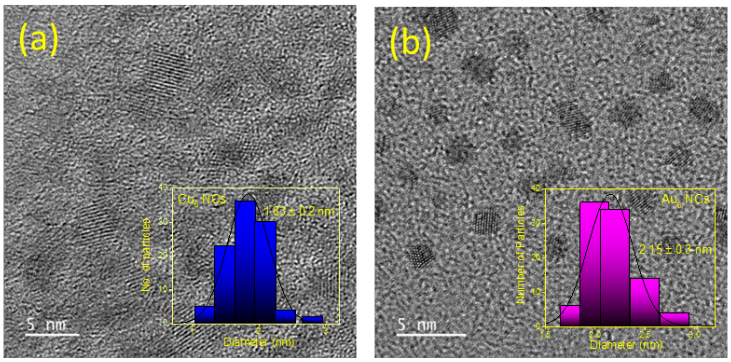

Figure S1: TEM image of (a) Cu_6 NCs (b) Au_6 NCs (Insets show the corresponding particle size distribution).

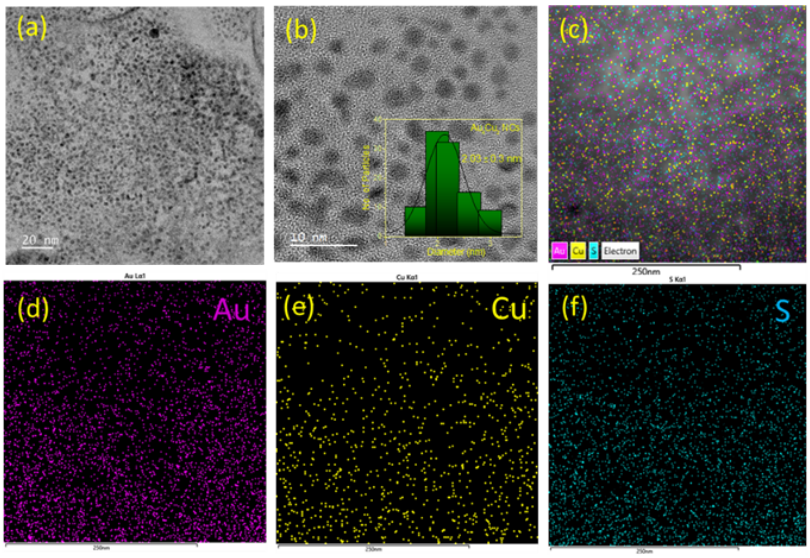

Figure S2: (a, b) TEM and HRTEM images of Au_4Cu_2 NCs (Inset shows the corresponding particle size distribution) and (c) corresponding elemental mapping showing the presence of d) Au e) Cu and f) S

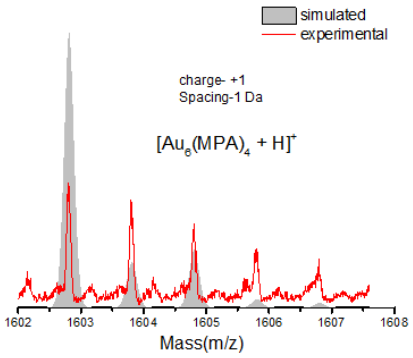

Figure S3: Isotopic Distribution (simulated and experimental) of peak * with formula $[Au_6(MPA)_4 + H]^+$

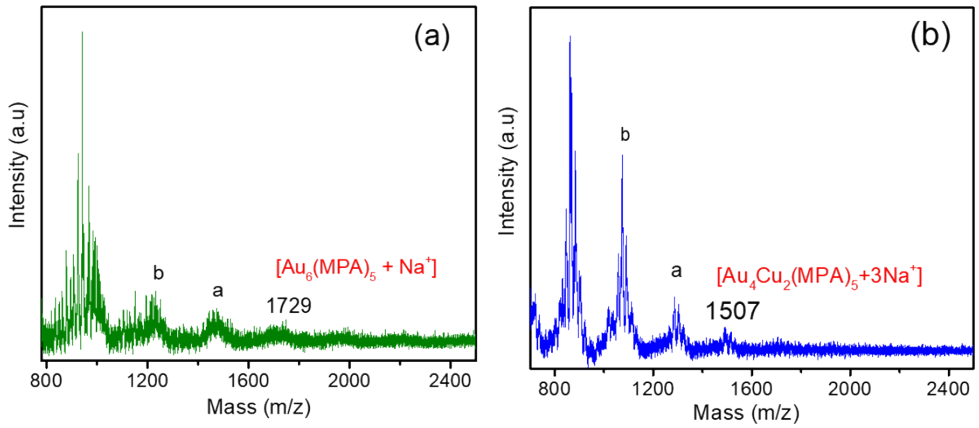

Figure S4: MALDI-MS analysis of (a) Au NCs and (b)AuCu NCs

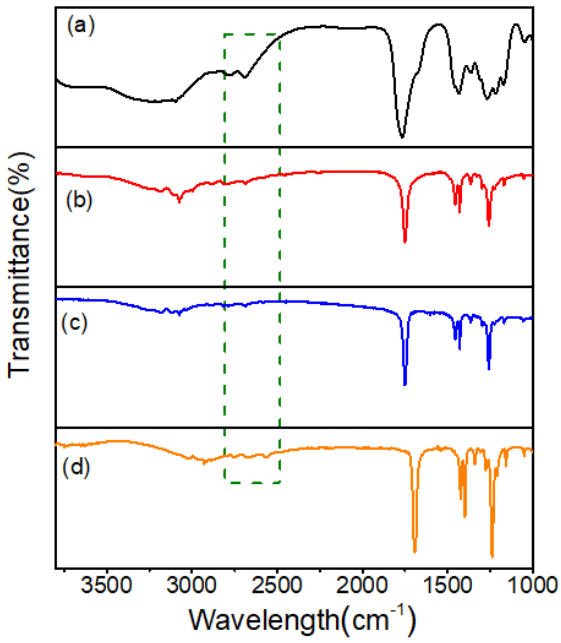

Figure S5: FTIR analysis of (a) MPA (b) Cu_6 NCs (c) Au_6 NCs, and (d) Au_4Cu_2 NCs

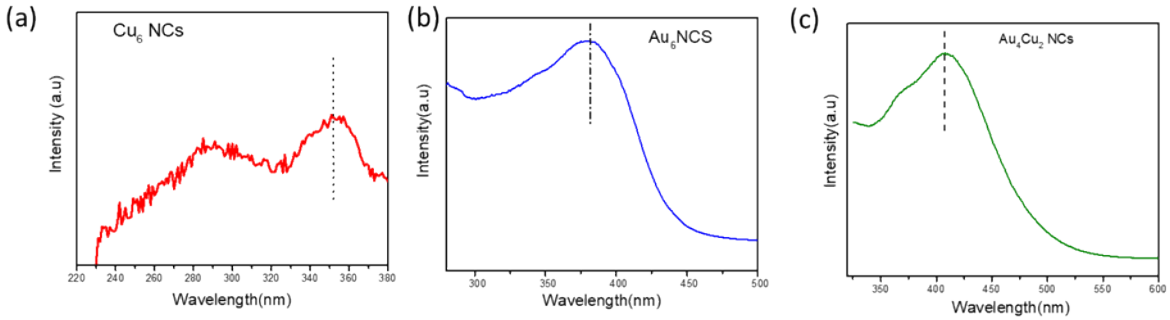

Figure S6: PLE spectra of (a)Cu_6 NCs (b) Au_6 NCs and (c) Au_4Cu_2 NCs

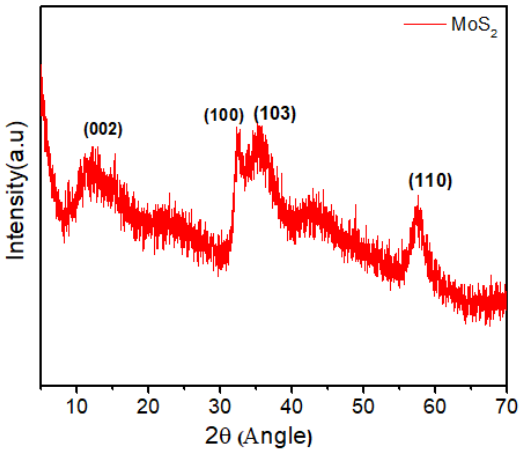

Figure S7: Powder X-ray Diffraction pattern of MoS_2

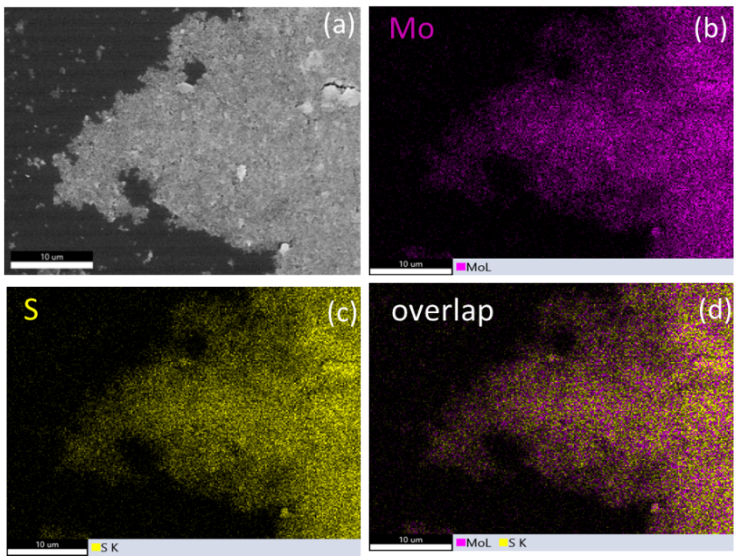

Figure S8: (a) SEM image of MoS_2 and corresponding elemental mapping of (b) Mo (c) S (d) overlap of Mo and S.

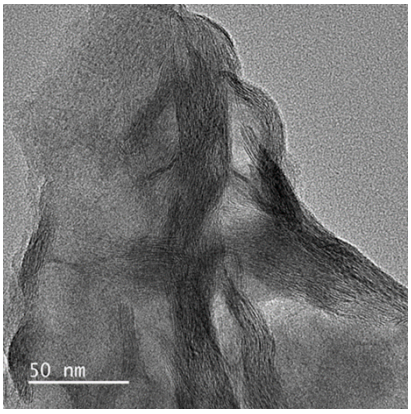

Figure S9: TEM image of MoS_2.

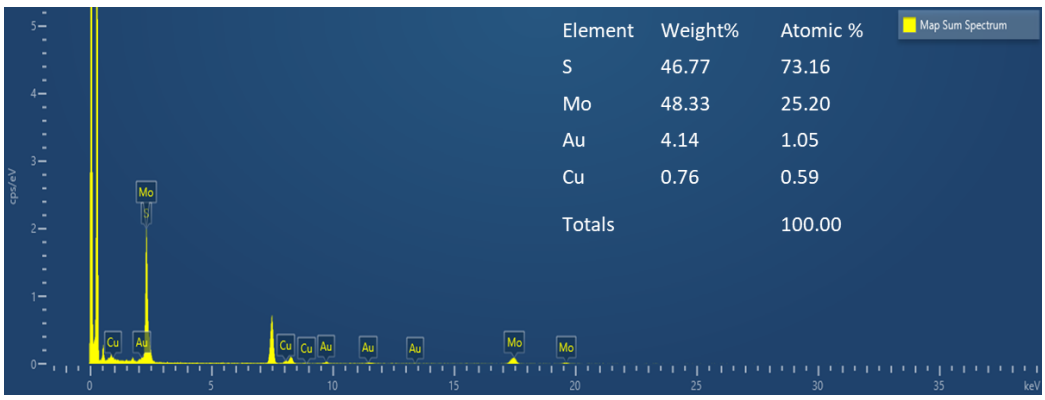

Figure S10: HRTEM-EDX spectrum of Au_4Cu_2/MoS_2 showing the presence of Au, Cu, Mo, and S (inset shows the contents of the elements).

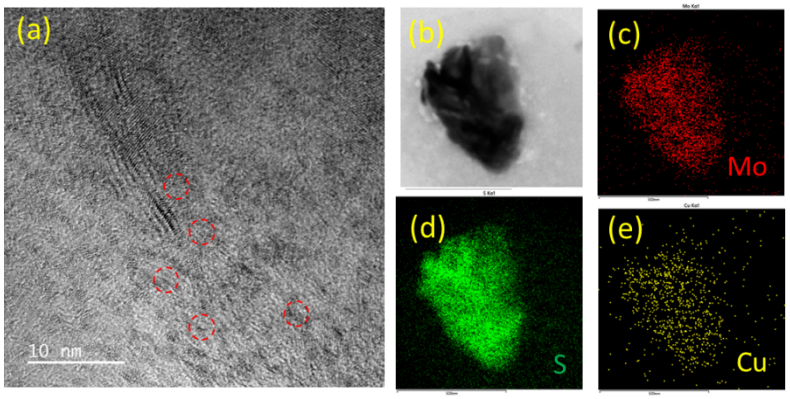

Figure S11: (a,b) TEM images of Cu/MoS_2 and (c) corresponding elemental mapping showing the presence of d) Mo e) S f) Cu

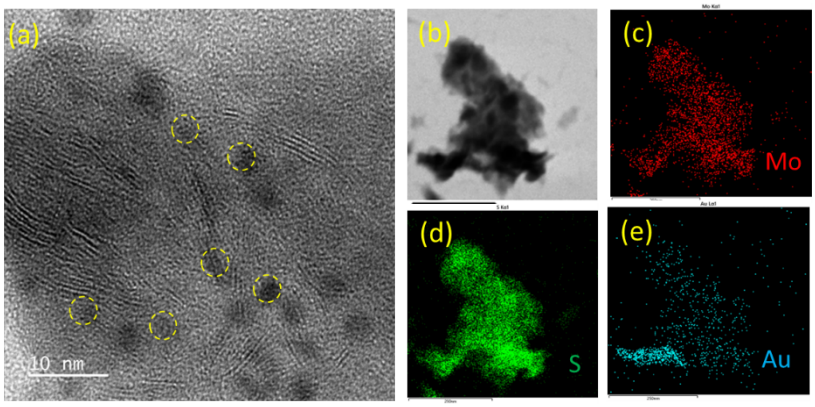

Figure S12: (a,b) TEM images of Au/MoS_2 and (c) corresponding elemental mapping showing the presence of d) Mo e) S f) Au

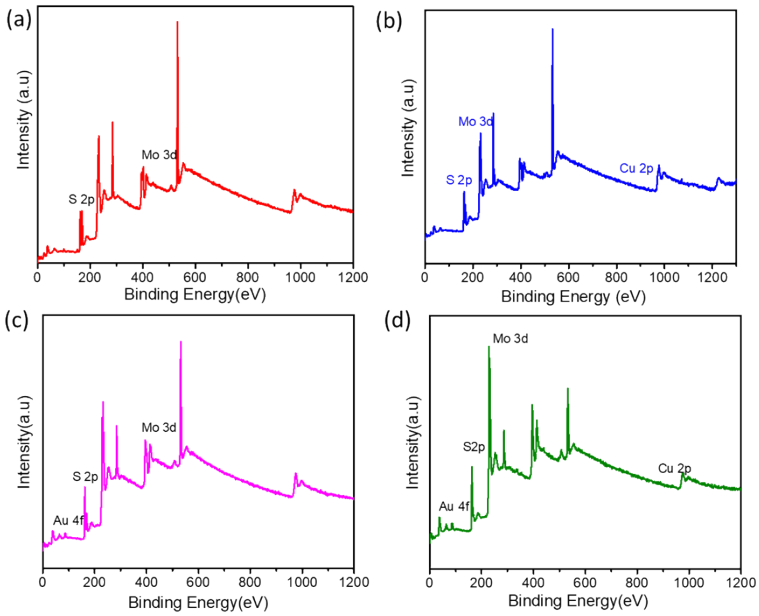

Figure S13: XPS survey spectrum of (a) MoS_2 (b) Cu_6/MoS_2 (c) Au_6/MoS_2 (d) and Au_4Cu_2/MoS_2

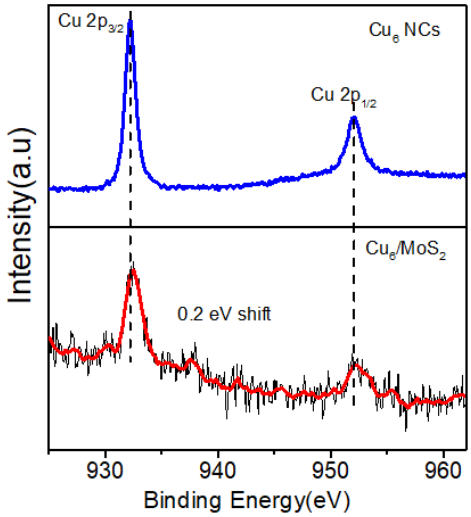

Figure S14: XPS analysis of Cu 2p in Cu_6 NCs and Cu_6/MoS_2 composite.

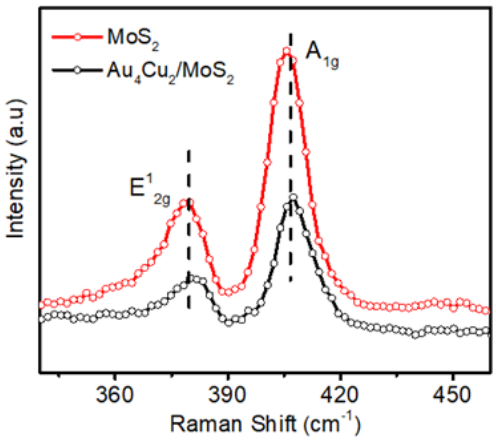

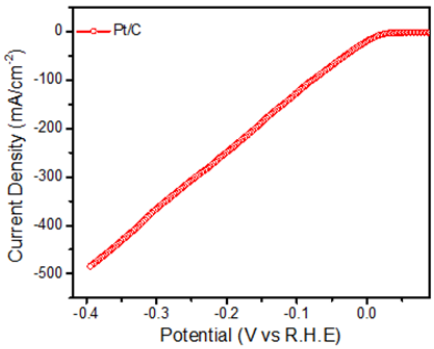

Figure S15: Raman spectra of MoS_2 and Au_4Cu_2/MoS_2

Figure S16: HER polarization curve of Pt/C.

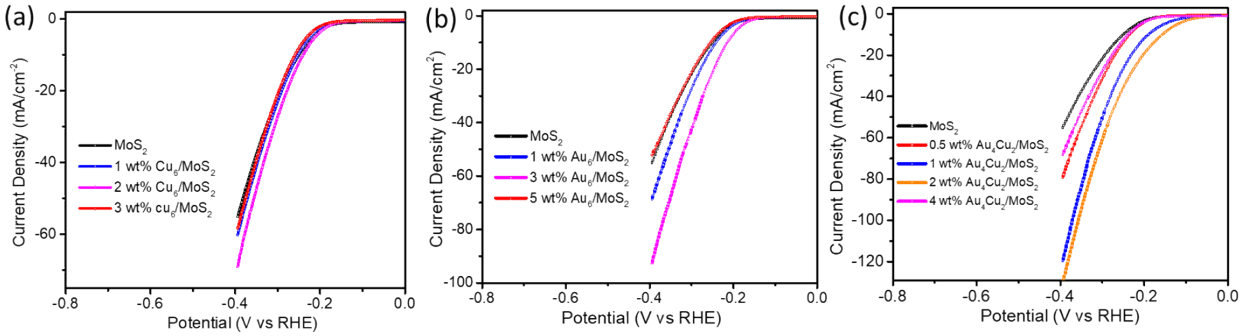

Figure S17 (a) HER polarization curve with different loadings recorded at a scan rate of 10 mV/sec of (a) Cu_6/MoS_2 (b) Au_6/MoS_2 and (c) Au_4Cu_2/MoS_2

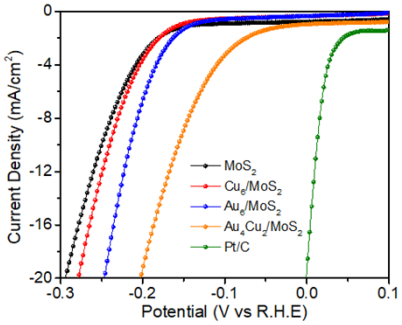

Figure S18: Polarization curves of NCs encapsulated over MoS_2 towards HER recorded at a scan rate of 10 mV/sec

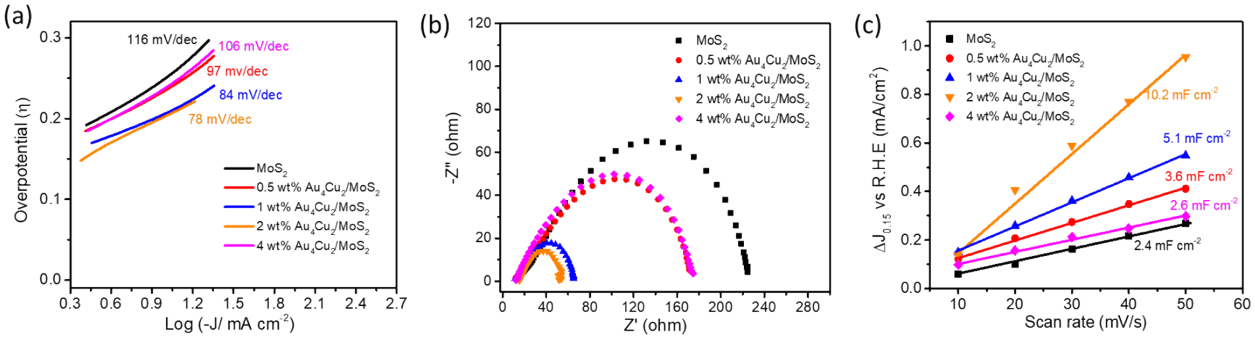

Figure S19: Electrocatalytic performance of Au_4Cu_2/MoS_2 with different loadings towards HER (a) Tafel slope derived from an early stage of HER polarization curve (b) Nyquist plots (c) Comparative C_{dl} plot as a function of scan rate.

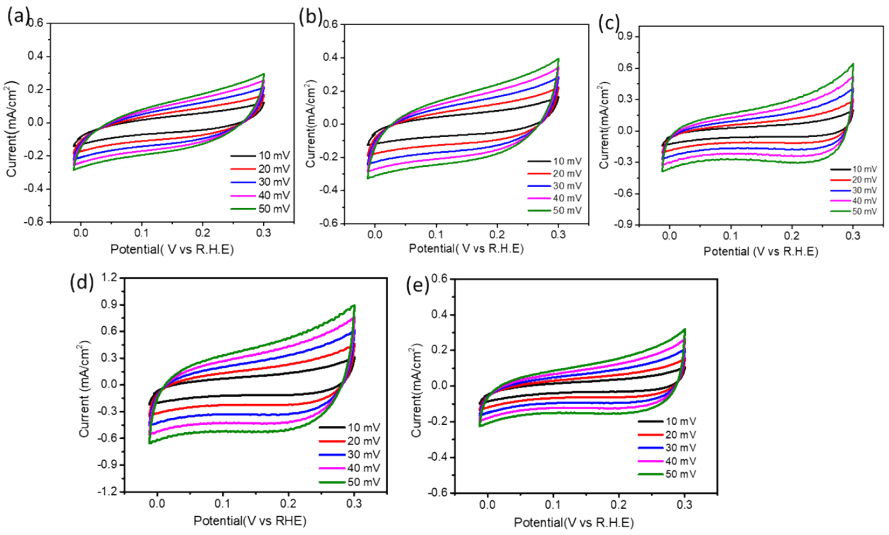

Figure S20: Cyclic voltammograms curve of (a) MoS_2 (b) 0.5 wt% Au_4Cu_2/MoS_2 (c) 1 wt% Au_4Cu_2/MoS_2 (d) 2 wt% Au_4Cu_2/MoS_2 (e) 4 wt% Au_4Cu_2/MoS_2 in the potential window of 0.0 V- 0.3 V vs. RHE at different scan rates.

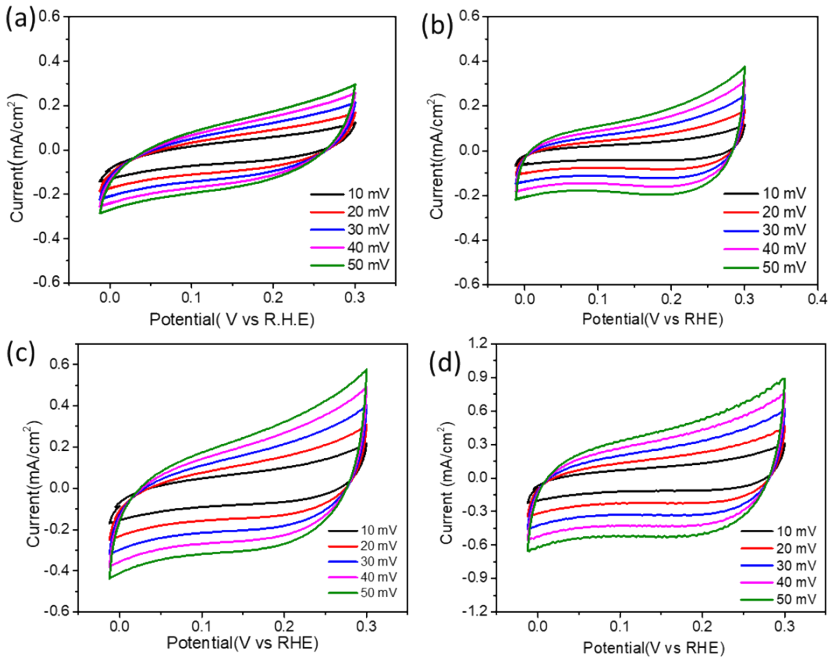

Figure S21: Cyclic voltammograms curve of (a) MoS_2 (b) Cu_6/MoS_2 (c) Au_6/MoS_2 (d) Au_4Cu_2/MoS_2 in the potential window of 0.0 V- 0.3 V vs. RHE at different scan rates.

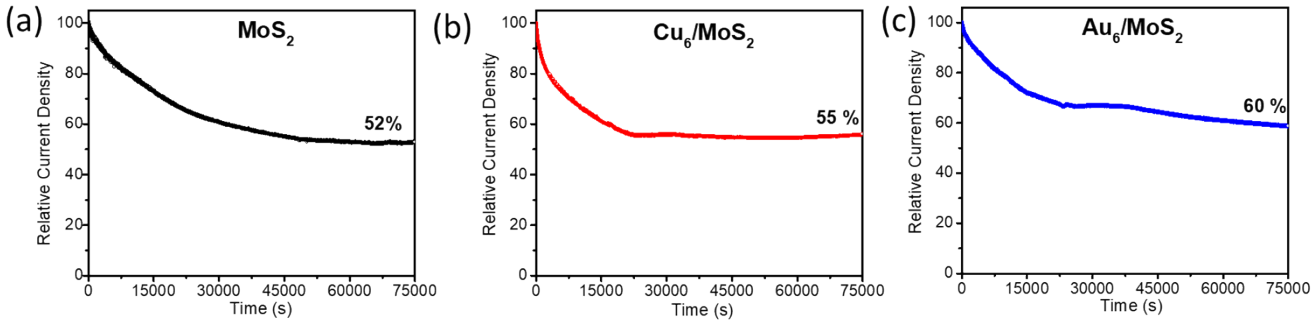

Figure S22: Chronoamperometry measurements of (a) MoS_2 (b) Cu_6/MoS_2 (c) Au_6/MoS_2

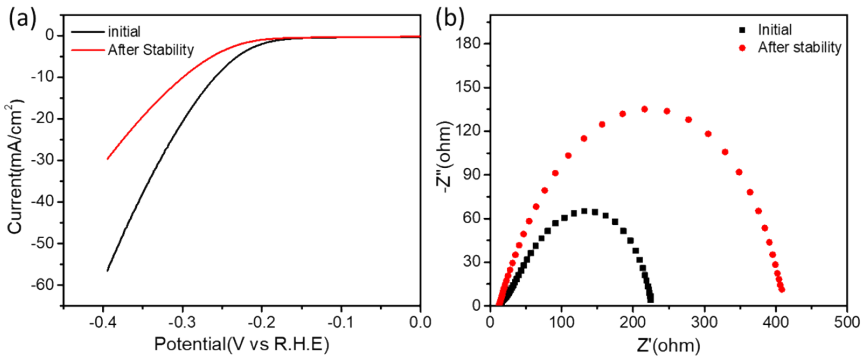

Figure S23: (a) HER polarization curve and (b) Nyquist plot curve of MoS_2 before and after stability test.

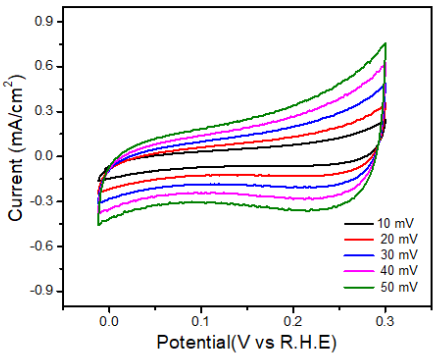

Figure S24: Cyclic voltammograms curve Au_4Cu_2/MoS_2 recorded after stability test.

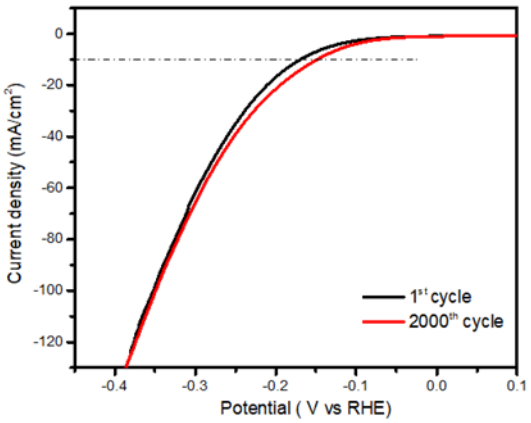

Figure S25: LSV cycling stability of Au_4Cu_2/MoS_2 upto 2000th LSV performance.

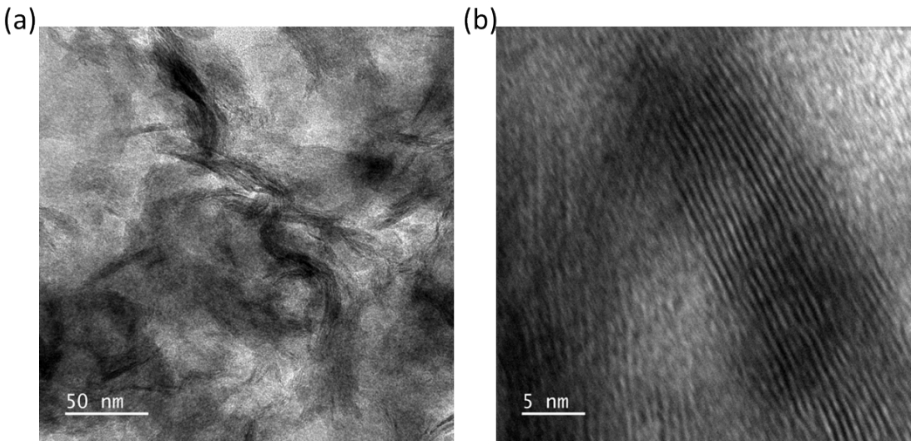

Figure S26: (a) TEM and (b) HRTEM images of Au_4Cu_2/MoS_2 after catalysis.

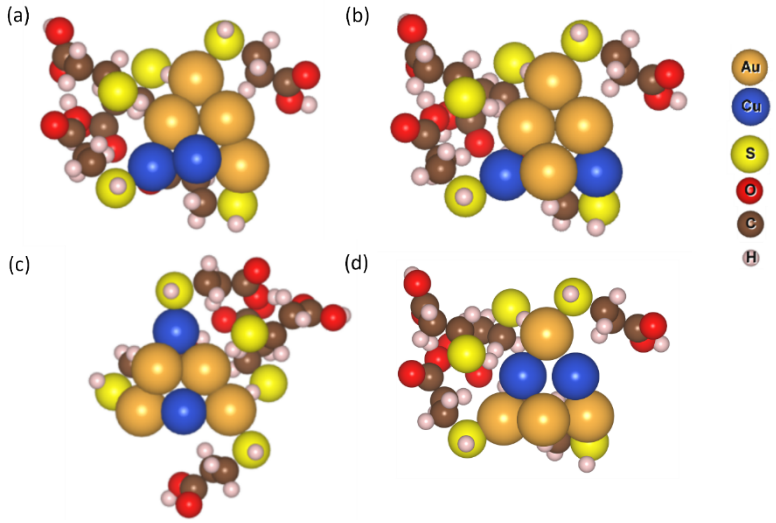

Figure S27: Possible arrangements of Cu and Au positions in $Au_4Cu_2(MPA)_5$ cluster named as: (a) A12, (b) A13, (c) A14 and (d) *A13*'.

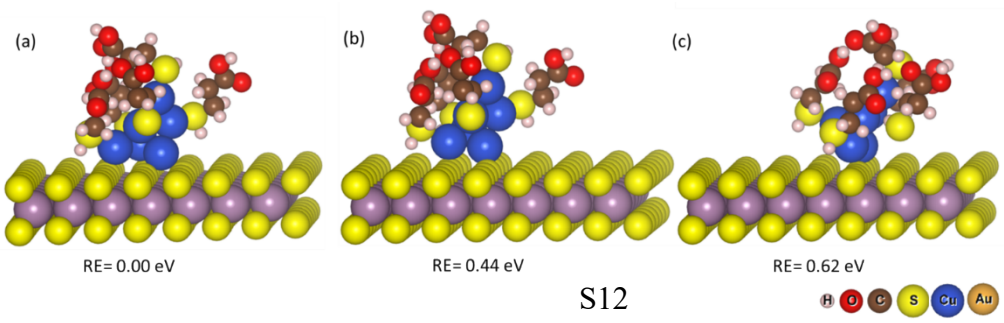

Figure S28: Side view of the possible orientations of $Cu_6(MPA)_5$ cluster on MoS_2 and their relative energies (RE).

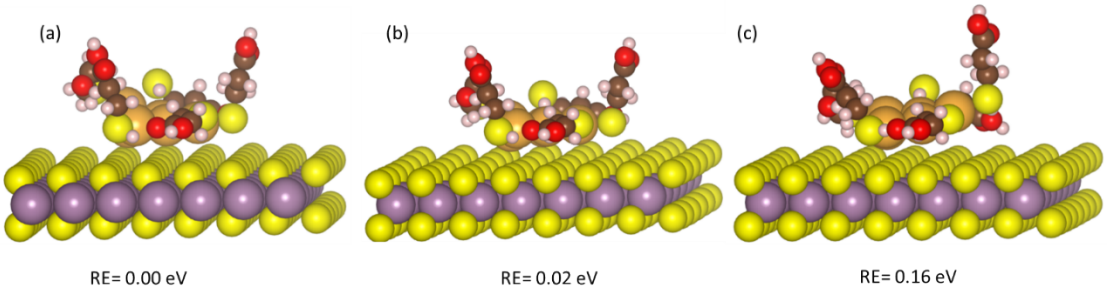

Figure S29: Side view of the possible sites of $Au_6(MPA)_5$ cluster on MoS_2 and their relative energies (RE).

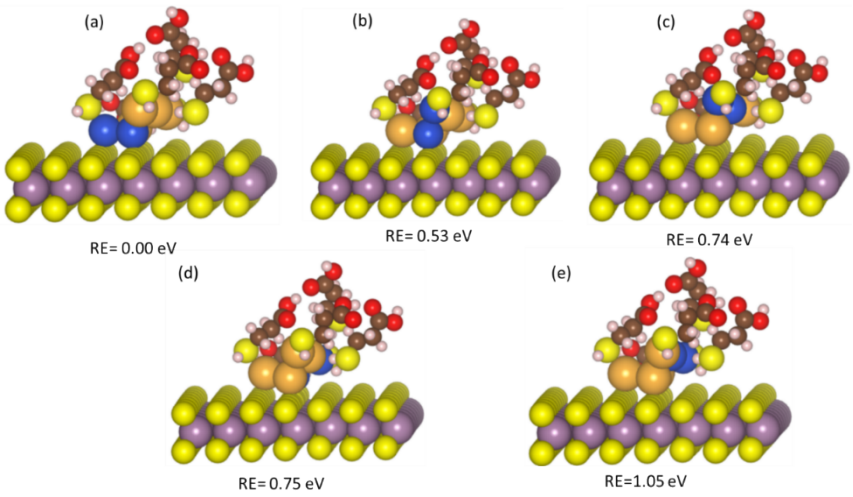

Figure S30: Side view of the possible orientations of $Au_4Cu_2(MPA)_5$ cluster on MoS_2 and their relative energies (RE).

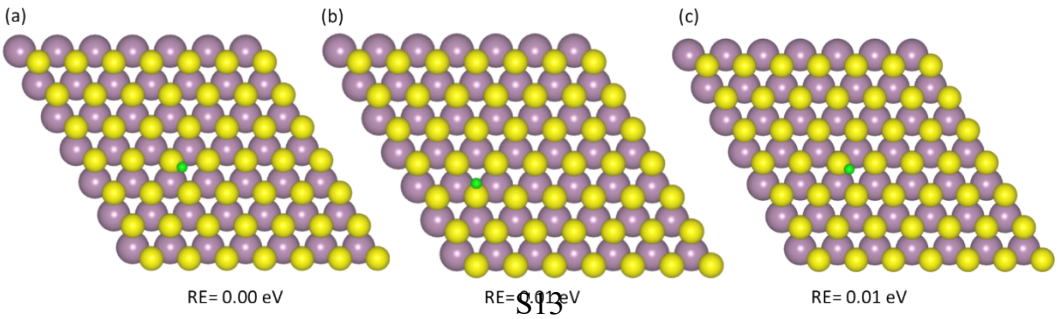

Figure S31: Top view of the possible orientations of MoS_2 for H-adsorption and their relative energies (RE).

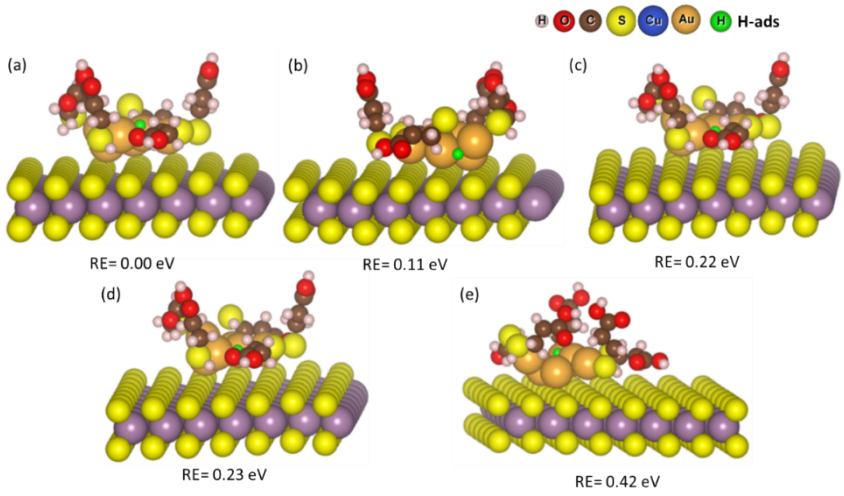

Figure S32: Side view of the possible orientations of H-adsorption on $Au_6(MPA)_5/MoS_2$ and their relative energies (RE).

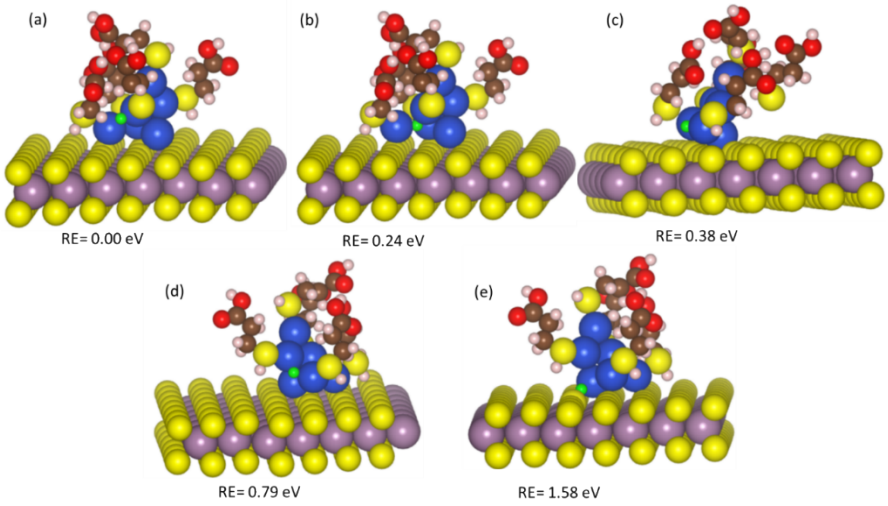

Figure S33: Side view of the possible orientations of H-adsorption on $Cu_6(MPA)_5/MoS_2$ and their relative energies (RE).

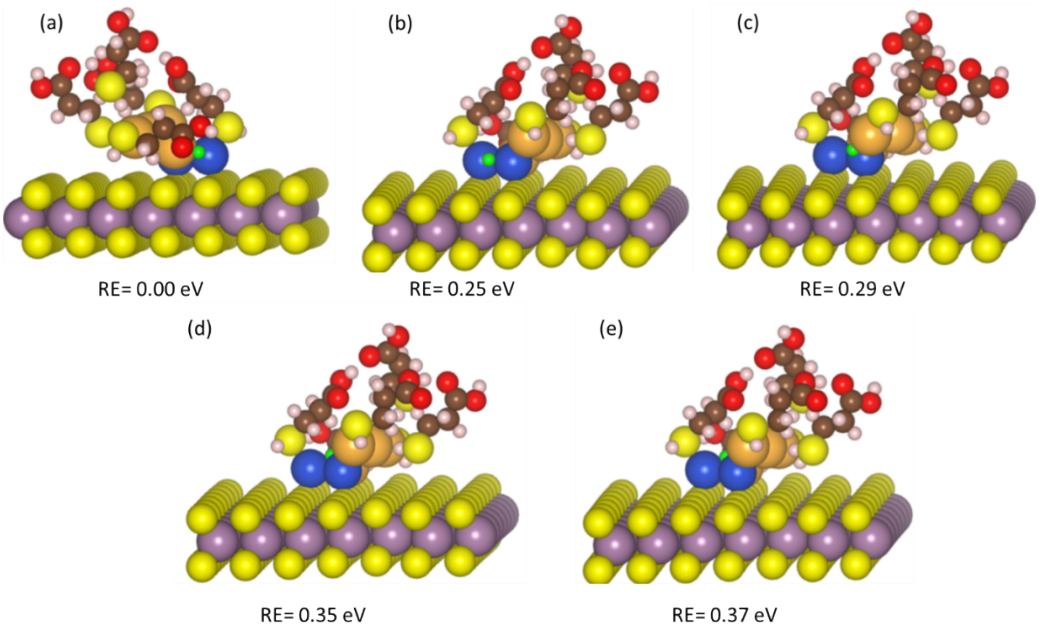

Figure S34: Side view of the possible orientations of H-adsorption on $Au_4Cu_2(MPA)_5/MoS_2$ and their relative energies (RE).

Table S1: Summary of HER overpotential, Tafel slope, double-layer capacitance, electrochemically active surface area, and charge-transfer resistance of Au_4Cu_2/MoS_2

Catalyst Name	**Electrolyte**	**Overpotential @10 mAcm^{-2} (mV)**	**Reference**
S-Au MoS_2 hybrid	0.5 M H_2SO_4	164	1
Ag/VA-MoS_2+20 min Pd G.R	0.5 M H_2SO_4	210	2
Au_{11} NCs/MoS_2	0.5 M H_2SO_4	292	3
Au_{25} NCs/MoS_2	0.5 M H_2SO_4	280	4
Au_2Pd_6 NCs/MoS_2	0.5 M H_2SO_4	225	5
$Au_{24}Ag_{20}$(t BuPh-CuC)$_{24}Cl_2$	0.5 M H_2SO_4	260	6
Ag NCs/MoS_2	0.5 M H_2SO_4	230	7
Pd_6 cluster/AC-V	0.5 M H_2SO_4	400	8
Pt NCs@ CIAC-121	0.5 M H_2SO_4	485	9
Au_4Cu_2 NCs/MoS_2	**0.5 M H_2SO_4**	**155**	**This work**

Sample	**Overpotential @ 10 mA/cm^{-2} (mV vs. RHE)**	**Tafel Slope (mv/dec)**	**Double layer capacitance C_{dl} (mF/cm^2)**	**Electrochemically active surface area, ECSA (cm^2)**	**Charge Transfer resistance, R_{ct} (ohm)**
MoS_2	252	116	2.4	60	210
0.5 wt% Au_4Cu_2/MoS_2	236	97	3.6	90	151
1 wt% Au_4Cu_2/MoS_2	192	84	5.1	127.5	54
2 wt% Au_4Cu_2/MoS_2	155	78	10.2	255	39
4 wt% Au_4Cu_2/MoS_2	238	106	2.6	65	162

Table S2: Comparison of Au_4Cu_2/MoS_2 catalyst with the state-of-the-art catalysts developed in the recent past.

References

1. R. Bar-Ziv, P. Ranjan, A. Lavie, A. Jain, S. Garai, A. Bar Hen, R. Popovitz-Biro, R. Tenne, R. Arenal, A. Ramasubramaniam, L. Lajaunie and M. Bar-Sadan, *ACS Appl. Energy Mater.*, 2019, **2**, 6043-6050.

2. I. Gerlitz, M. Fiegenbaum-Raz, M. Bar-Sadan, H. Cohen, A. Ismach and B. A. Rosen, *ChemElectroChem*, 2020, **7**, 4224-4232.

3. S. Gratious, A. Karmakar, D. Kumar, S. Kundu, S. Chakraborty and S. Mandal, *Nanoscale*, 2022, **14**, 7919-7926.

4. S. Zhao, R. Jin, Y. Song, H. Zhang, S. D. House, J. C. Yang and R. Jin, *Small*, 2017, **13**, 1701519.

5. Y. Du, J. Xiang, K. Ni, Y. Yun, G. Sun, X. Yuan, H. Sheng, Y. Zhu and M. Zhu, *Inorg. Chem. Front.*, 2018, **5**, 2948-2954.

6. Y. Tang, F. Sun, X. Ma, L. Qin, G. Ma, Q. Tang and Z. Tang, *Dalt.Trans.*, 2022, **51**, 7845-7850.

7. M. Ghosal Chowdhury, L. Sahoo, S. Maity, D. Bain, U. K. Gautam and A. Patra, *ACS Appl. Nano Mater.*, 2022, **5**, 7132-7141.

8. X. Gao and W. Chen, *Chem. Commun.*, 2017, **53**, 9733-9736.

9. S. Wang, X. Gao, X. Hang, X. Zhu, H. Han, W. Liao and W. Chen, *J. Am. Chem. Soc.*, 2016, **138**, 16236-16239.